JVST A
Journal of Vacuum Science & Technology A

Hydrogen desorption kinetics for aqueous hydrogen fluoride and remote hydrogen plasma processed silicon (001) surfaces

Cite as: J. Vac. Sci. Technol. A **33**, 05E115 (2015); https://doi.org/10.1116/1.4926733
Submitted: 17 May 2015 • Accepted: 26 June 2015 • Published Online: 20 July 2015

Sean W. King, Robert F. Davis, Richard J. Carter, et al.

Hydrogen desorption kinetics for aqueous hydrogen fluoride and remote hydrogen plasma processed silicon (001) surfaces

Sean W. King[a)] and Robert F. Davis[b)]
Department of Materials Science and Engineering, North Carolina State University, Raleigh, North Carolina 27695

Richard J. Carter,[c)] Thomas P. Schneider,[d)] and Robert J. Nemanich[e)]
Department of Physics, North Carolina State University, Raleigh, North Carolina 27695

(Received 17 May 2015; accepted 26 June 2015; published 20 July 2015)

The desorption kinetics of molecular hydrogen (H_2) from silicon (001) surfaces exposed to aqueous hydrogen fluoride and remote hydrogen plasmas were examined using temperature programmed desorption. Multiple H_2 desorption states were observed and attributed to surface monohydride (SiH), di/trihydride ($SiH_{2/3}$), and hydroxide (SiOH) species, subsurface hydrogen trapped at defects, and hydrogen evolved during the desorption of surface oxides. The observed surface hydride species were dependent on the surface temperature during hydrogen plasma exposure with mono, di, and trihydride species being observed after low temperature exposure (150 °C), while predominantly monohydride species were observed after higher temperature exposure (450 °C). The ratio of surface versus subsurface H_2 desorption was also found to be dependent on the substrate temperature with 150 °C remote hydrogen plasma exposure generally leading to more H_2 evolved from subsurface states and 450 °C exposure leading to more H_2 desorption from surface SiH_x species. Additional surface desorption states were observed, which were attributed to H_2 desorption from Si (111) facets formed as a result of surface etching by the remote hydrogen plasma or aqueous hydrogen fluoride treatment. The kinetics of surface H_2 desorption were found to be in excellent agreement with prior investigations of silicon surfaces exposed to thermally generated atomic hydrogen.
[http://dx.doi.org/10.1116/1.4926733]

I. INTRODUCTION

Hydrogen is ubiquitous throughout all silicon microelectronic fabrication processes including epitaxy,[1] oxidation,[2] etching,[3] cleaning,[4,5] chemical mechanical polishing,[6] gate oxide passivation,[7] contact formation,[8] and metallization.[9] Accordingly, numerous ultrahigh vacuum (UHV) studies of the interaction of hydrogen with atomically clean Si (001) and (111) surfaces have been performed.[10–19] While such UHV studies have provided a greater fundamental understanding of the interaction of hydrogen with silicon surfaces, they have largely been performed under conditions far removed from those of typical semiconductor processes.[1] In this regard, we have utilized temperature programmed desorption (TPD) to investigate the interaction of hydrogen with Si (001) surfaces under conditions more representative of semiconductor processes via *ex-situ* exposure to aqueous hydrogen fluoride (HF) and atomic hydrogen from an *in-situ* remote hydrogen plasma operated under milliTorr conditions.[20,21] Aqueous HF and related solutions are utilized throughout silicon semiconductor device fabrication for a variety of surface cleaning and etching processes.[4] Similarly, remote hydrogen plasmas have received significant research interest for cleaning of Si (Ref. 5) and other surfaces[22–25] and are now utilized in a variety of applications throughout the semiconductor industry.[26,27]

It has been shown that molecular hydrogen (H_2) has essentially a zero sticking coefficient ($S \leq 10^{-8}$) on atomically clean Si surfaces, while thermally generated atomic hydrogen (H) has an initial adsorption sticking coefficient (S_0) of 1 that decreases with increasing coverage (θ) according to a $S = 1 - \theta$ relationship.[15] For UHV prepared, atomically clean Si (001)–(2 × 1) surfaces exposed at room temperature to thermally generated atomic hydrogen, silicon monohydride (SiH) species form initially up to a coverage of 1 monolayer (ML = 6.78×10^{14} atoms/cm^2).[28] At higher hydrogen exposures and coverage, the (2 × 1) reconstruction converts to (3 × 1) due to Si–Si dimer cleavage and silicon dihydride formation (SiH_2).[29] At a saturation coverage of 1.8–2.0 ML, trihydride species form on the Si (001) surface and the symmetry converts to (1 × 1).[30]

On heating such hydrogen saturated (1 × 1) surfaces, the trihydride species first desorb primarily as SiH_4 and H_2 via a β_3 desorption state at ~375 °C.[10,15] The kinetics for the β_3 SiH_3/SiH_4 desorption have been reported to be first order with an activation energy of 1.35 eV.[31] At higher temperatures, hydrogen desorption from the dihydride and monohydride species occur as molecular H_2 via β_2 and β_1 states

a)Present address: Logic Technology Development, Intel Corporation, Hillsboro, OR 97124; electronic mail: sean.king@intel.com
b)Present address: Department of Materials Science and Engineering, Carnegie Mellon University, Pittsburgh, PA 15260.
c)Present address: GLOBALFOUNDRIES, 400 Stone Break Extension, Malta, NY 12020.
d)Present address: 3 Pendleton Court, Durham, NC 27713.
e)Present address: Department of Physics, Arizona State University, Tempe, AZ 85287.

at temperatures of ~425 and 520 °C, respectively.[10,11] The kinetics of β_2 H_2 desorption from dihydride species on Si (001) surfaces have been studied in less detail with only one report of second order kinetics with an activation energy of ~1.9 eV.[13] In contrast, the kinetics of β_1 H_2 desorption from monohydrides on Si (001) surfaces has been studied by numerous investigators and demonstrated to be first order with an activation energy of 2.0–2.5 eV.[32] More detailed studies by Narita, however, have shown that for Si (001) surfaces the β_1 state is actually composed of two peaks.[33–35] At low hydrogen coverage ($\theta < 0.4$ ML), the lower temperature β_{1a} peak exhibits first order kinetics with $E_d = 1.6\,eV \pm 0.1\,eV$ ($\nu = 7.7 \pm 4.1 \times 10^8\ s^{-1}$), while the higher temperature β_{1b} peak exhibits second order kinetics with $E_d = 1.8 \pm 0.1\,eV$ ($\nu = 4 \times 3 \times 10^{11}\ ML^{-1}s^{-1}$).[33] The lower temperature β_{1a} peak was attributed to H_2 desorption from doubly occupied Si dimers (DOD), while the higher temperature β_{1b} peak was attributed to H_2 desorption from singly occupied dimers (SOD).[34,35]

In addition to surface silicon hydride species, UHV investigations of the interaction of thermally generated atomic hydrogen with Si (001) surfaces have identified the presence of several other desorption states.[36–39] Specifically, Hess has observed H_2 desorption states at 330–360 °C just below the β_2-dihydride state at 425 °C.[36] These states were attributed to H_2 desorption from subsurface B-H complexes formed with the boron p-type dopant during atomic hydrogen exposure.[40–42] The uptake of these lower temperature desorption states increased with the sample temperature during atomic hydrogen dosing, suggesting an activation barrier for subsurface H_2 uptake. Kim observed similar behavior for boron doped Si (001) where *in-situ* H_2 TPD of boron doped GSMBE Si (001) epilayers showed desorption states at 330 and 470 °C in addition to the β_2 and β_1 states at 405 and 515 °C, respectively.[37] In this case, the authors attributed the additional states to desorption from SiH_2 and SiH surface species with boron back bonds. Foo has reported a similar effect, where an H_2 desorption state at 480 °C was attributed to desorption from SiH states with carbon back bonds.[38] Lastly, Hess has shown that surface roughening induced by Kr^+ ion bombardment can lead to increased dihydride formation with a saturation surface coverage in excess of 2 ML.[39]

Investigations of hydrogenated Si surfaces prepared via various *ex-situ* aqueous treatments have also been reported.[43–46] These studies have shown that aqueous HF and NH_4F mixtures can produce hydrogen terminated surfaces with various concentrations of mono, di, and trihydride species. The exact concentration of the species is dependent on the HF concentration, *p*H, and Si orientation. As an example, Hiroshita and others have observed that the β_1 and β_2 desorption states from boron doped, *p*-type Si (001) surfaces treated with 1%–5% HF solutions exhibit similar intensities.[47] This is analogous to the hydrogenated Kr^+ ion bombarded Si (001) surfaces in the study by Hess[39] and has been demonstrated by Thanh to be due to roughening of the Si (001) surface by the HF solution.[48]

In this study, we specifically demonstrate that the coverage and desorption kinetics of hydrogen species formed on Si (001) surfaces by aqueous HF and remote hydrogen plasma treatments exhibit both some similarities and differences relative to those for Si surfaces prepared and exposed to thermally generated atomic hydrogen under pure UHV conditions. Si (001) surfaces exposed to either thermal or remote plasma generated atomic hydrogen both exhibit desorption states that can be attributed to mono, di, and trihydride surface species. The differences are related primarily to the relative coverage of Si-H and $SiH_{2/3}$ surface species and the appearance of additional desorption states that are attributed to subsurface species and (111) surface facets formed during the various remote H-plasma conditions investigated. We also observed in this study the evolution of hydrogen during desorption of surface oxide contamination unintentionally formed during the remote H-plasma exposure. The kinetics for hydrogen desorption from all the various surface species were determined via a detailed kinetic analysis and compared to prior investigations of hydrogen desorption from Si (001) exposed to thermally generated hydrogen.

II. EXPERIMENT

The substrates and sample preparation procedures used in these experiments have been described in detail elsewhere;[49–51] however, a brief overview is presented herein. The Si (001) wafers utilized in these experiments were phosphorous doped, *n*-type with a resistivity of 5–10 Ω cm. These wafers were first given a UV/ozone clean followed by a HF/alcohol spin clean and then immediately loaded into a vacuum loadlock.[52] For comparison, one sample was given a UV/ozone clean followed by dipping in dilute (10:1) HF. The thus prepared Si (001) wafers were exposed to atomic hydrogen (and various charged species) generated from an inductively coupled, remote plasma system attached to the vacuum load lock via a UHV transfer line.[20,21] To generate a range of hydrogen surface species and coverage, the time and temperature of the remote hydrogen plasma exposure was varied from 2 to 60 min and 150 to 450 °C, respectively.

The process gases in the remote plasma system flowed through a quartz tube mounted at the top of the chamber. The samples were located 40 cm below the center of the RF coil. An in-line purifier and filter was used for further purification of the hydrogen. Sample heating in the plasma system was achieved using a tungsten filament heater as previously described.[53] The H_2 plasma was operated at 20 W and 15 mTorr.[20] At this pressure, the plasma was largely confined upstream of the sample, but a weak diffuse glow was observed in the sample vicinity. Prior characterization of the H_2 plasma has shown it to consist primarily of H, H^+, H_2, and electrons. H_2 to H dissociation efficiencies and H^+/H ratios of 50% and 10^{-4}, respectively, have been previously estimated for these plasma conditions.[20] The H flux to the surface was $\sim 10^{16}\,cm^{-2}\,s^{-1}$. The plasma density was $\sim 10^8\,cm^{-3}$, and the ion flux was $\sim 10^{12}\,cm^{-2}\,s^{-1}$. The energy of the ions in the plasma is low with an average characteristic energy of ~223 °C.[20]

TPD measurements were performed on both the *ex-situ* wet chemical HF and *in-situ* remote H-plasma treated Si (001) surfaces using a UHV gas-source molecular beam epitaxy (GSMBE) system designed for atomic layer epitaxy of SiC thin films and attached to the same UHV transfer line as the remote hydrogen plasma system.[53,54] For the TPD measurements, the GSMBE was equipped with a Hiden Analytical 0–200 atomic mass unit (amu) quadrupole mass spectrometer (QMS) fitted inside a differentially pumped chamber having a 0.5 cm diameter opening.[53] During the TPD measurements, the sample holder/heater was positioned <1 cm from the front of the QMS opening. The TPD experiments were conducted to a maximum temperature of ~1000 °C using a heating rate of 20–60 °C/min generated by a W filament heater positioned behind the Si wafer. During each TPD measurement, the QMS solely monitored $m/e^- = 2$ (H_2) to maximize the data acquisition rate.[54]

To calibrate the hydrogen desorption signal from the remote hydrogen plasma treated Si (001) surfaces, hydrogen desorption from a Si (111)–(7 × 7) surface exposed to a saturation dose of atomic hydrogen from a hot rhenium filament inside the GSMBE was also examined.[54] The saturation surface coverage of hydrogen from a Si (111) surface has been previously determined to be 1.25 monolayer (ML = 7.8 $\times 10^{14}/cm^2$) by Culbertson *et al.*[55] By equilibrating the area under the H_2 TPD spectra from a saturated Si (111) surface to $8.75 \times 10^{14}/cm^2$, we were able to calibrate the hydrogen desorption intensity against a known standard. As the definition of ML is different for Si (001) and (111) orientations, all hydrogen coverage values are reported as ML Si (001) and calculated as 7.8/6.8 × Si (111) ML.

To ensure that all the desorbed species originated only from the substrate and not from other surfaces (e.g., sample heater), TPD measurements were also performed on clean and thoroughly degassed Si wafers prior to TPD measurements on the remote hydrogen plasma treated Si samples. In these experiments, none of the desorption features observed in the remote hydrogen plasma treated measurements were noticed. Detection of species desorbing from the molybdenum sample holder was minimized by the designed geometry of the experiment. Specifically, line of sight desorption of species from the molybdenum sample holder into the QMS was greatly minimized by the large diameter of the Si sample substrate (2.54 cm) and the significantly smaller QMS chamber opening (0.5 cm).[53,54]

Additional spurious effects may also occur in TPD experiments such as electron stimulated desorption (ESD) of H caused by electrons from the mass spectrometer ionizer.[56] While enclosing the mass spectrometer in the differentially pumped chamber may help to minimize this effect, we were not able to independently bias the chamber opening to completely eliminate this effect. Thus, some ESD effects may be present in our data. However, we feel this effect would only contribute to our background H_2 signal and not significantly alter our conclusions.

Kinetic treatments of TPD spectra normally use the Polanyi–Wigner desorption rate equation[57,58]

$$-d\theta/dt = \text{desorption rate (DR)} = \nu_d \theta^n \exp(-E_d/RT), \quad (1)$$

where θ = surface coverage, ν_d = desorption jump frequency/pre-exponential, n = rate order, and E_d = desorption activation energy. In principal, ν_d, n, and E_d can all be dependent on θ; however, most analyses assume these parameters to be independent of θ. Using the latter approach and taking the logarithm of both sides of the above equation accompanied by mathematical rearrangement, one obtains

$$\ln(DR) - n\ln\theta = \ln\nu_d - E_d/RT, \quad (2)$$

where if the correct rate order (n) is chosen, a plot of (ln (DR) − nlnθ) vs (1/T) yields a straight line and has a slope of $-E_d/R$ and a y-intercept of $\ln\nu_d$. The mathematical methods used for analyzing (ln (DR) − nlnθ) vs (1/T) were identical to those of Parker *et al.*[58] Once n, ν, and E_d were determined from the above analysis, fits to the experimental data were generated by simply plotting $d\theta/dt$ using the Polanyi–Wigner equation and the extracted kinetic parameters.

In-situ Auger electron spectroscopy (AES) and low energy electron diffraction (LEED) measurements were also performed before and after each TPD measurement to monitor changes in surface structure and chemical composition. The LEED and AES measurements were performed using a separate vacuum system attached to the GSMBE and remote H-plasma system via the same UHV transfer line.[49] The AES spectra were obtained using a beam energy of 3 keV, collected in the undifferentiated mode and numerically differentiated. LEED patterns were observed using an 80 eV, 1 mA beam.[51]

III. RESULTS AND DISCUSSION

A. Overview of results

In Fig. 1, we present an overview of five representative H_2 TPD spectra collected from Si (001) wafers after the *ex-situ* UV/ozone and HF surface cleaning and after *in-situ* remote H-plasma exposures performed for various times and substrate temperatures. The spectra exhibit many similarities and substantial differences. To make the similarities more apparent, we have included in Fig. 1 markers for the approximate positions of the β_1, β_2, and β_3 H_2 desorption states based on prior TPD investigations of hydrogenated Si surfaces prepared via *ex-situ* HF and/or *in-situ* thermally generated atomic H. Although the pre-TPD LEED patterns differed significantly for each of the spectra illustrated in Fig. 1, (2 × 1) LEED patterns were observed after TPD in all cases (see Table I). Similarly, pre-TPD AES measurements showed substantial variation in surface oxygen contamination (ranging from < 0.03 ML to > 5 ML). However, all post-TPD AES measurements showed < 0.05 ML oxygen contamination. Surface carbon contamination was constant at < 0.02 ML pre/post-TPD.

Focusing on the H_2 TPD spectrum collected from a Si (001) wafer that received only an *ex-situ* UV/ozone and 10:1

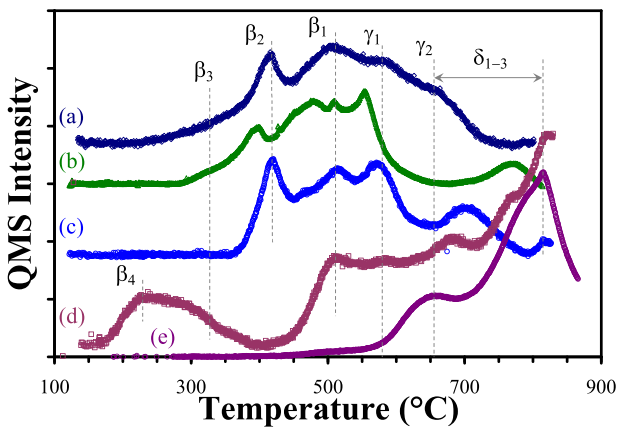

FIG. 1. (Color online) H_2 TPD spectra from Si (001) wafers after (a) *ex-situ* UV/ozone and 10:1 HF dip cleaning, or *ex-situ* UV/ozone and HF/alcohol spin cleaning followed by *in-situ* remote H-plasma processing at (b) 150 °C for 2 min, (c) 150 °C for 60 min, (d) 450 °C for 2 min, and (e) 450 °C for 60 min.

HF dip clean [Fig. 1(a)], one can clearly distinguish the β_1, β_2, and β_3 H_2 desorption states, respectively, at 510, 415, and 350 °C, respectively, consistent with prior studies of phosphorous doped, *n*-type Si (001).[59] Similar to Hirashita,[47] we also observed the intensity of the β_1 and β_2 states from the 10:1 HF dip cleaned Si (001) surfaces to be roughly equivalent. Based on the results of Thanh,[48] this indicates some roughening of the Si (001) surface by the HF treatment. In addition to the β_{1-3} states, we observed continued H_2 desorption at higher temperatures beyond the β_1 state (labeled $\gamma_{1,2}$ and δ_{1-3}). Such higher temperature H_2 desorption states were observed for all of the H_2 TPD spectra collected from the Si (001) samples that were additionally exposed to the *in-situ* remote H-plasma.

The origin of the higher temperature desorption states observed in all the TPD spectra will be discussed further later, but can be tentatively attributed to the release of hydrogen from residual carbon, oxygen, or fluorine surface contamination. For the former, we note that similar higher temperature desorption peaks have also been observed by others for Si wafers hydrogenated *ex-situ* using aqueous HF/NH_4F chemistries.[46,60–62] In this case, Pietsch[49] has shown for Si (111) and Kawase[60] for Si (001) surfaces cleaned in HF solutions that decomposition of carbon-hydride organic surface contaminants can lead to a broad H_2 desorption peak from 300 to 700 °C (peaking at ~450 °C). In addition, Pietsch has shown using hydrophilic Si (111) surfaces cleaned in NH_4OH:H_2O_2:H_2O solutions that the decomposition of surface silanol groups (Si-OH) can lead to broad H_2 and H_2O desorption from (200–700 °C) followed by a rapid increase starting at 900 °C. Lastly, Tomita[61] and Kinoshita[62] have observed H_2 TPD peaks at 580–600 °C that correlated with the desorption of F_2 and various SiF_x species in the same temperature range.

TABLE I. Summary of LEED and AES data.

Process	LEED	AES O contamination
UV/ozone and HF	Pre-TPD: (1 × 1)	Pre-TPD: <0.03–0.1 ML
	Post-TPD: (2 × 1)	Post-TPD: <0.05 ML
Remote H-plasma: 150 °C, 2 min	Pre-TPD: (1 × 1)	Pre-TPD: <0.05–0.1 ML
	Post-TPD: (2 × 1)	Post-TPD: <0.05 ML
Remote H-plasma: 150 °C, 60 min	Pre-TPD: Diffuse (1 × 1)	Pre-TPD: <0.05–0.1 ML
	Post-TPD: (2 × 1)	Post-TPD: <0.05 ML
Remote H-plasma: 450 °C, 2 min	Pre-TPD: (2 × 1)	Pre-TPD: <0.1–0.3 ML
	Post-TPD: (2 × 1)	Post-TPD: <0.05 ML
Remote H-plasma: 450 °C, 60 min	Pre-TPD: None	Pre-TPD: >5 ML
	Post-TPD: (2 × 1)	Post-TPD: <0.05 ML

In this regard, we note that fluorine was not detected in AES measurements of the Si (001) wafers post the *ex-situ* UV/ozone and HF cleans, but as noted by Pietsch, AES generally has a relatively poor sensitivity to fluorine due to ESD effects. For the same surfaces though, some carbon and oxygen contamination was observed with ≤0.03 ML for the UV/ozone and HF/alcohol spin cleaned surfaces and ≤0.1 ML for the UV/ozone and 10:1 HF dip cleaned surfaces. This level of contamination is consistent with the levels previously described by Pietsch for similarly processed Si (111) substrates.[46] For the TPD spectrum of the UV/ozone and HF/alcohol cleaned surface [see Fig. 2(b)], greatly diminished H_2 desorption above the β_1 state was observed with only a small peak at ~580 °C that we label γ_1. However, for the UV/ozone and 10:1 HF dip clean surface with higher oxygen contamination (~0.1 ML), greatly increased H_2 desorption above the β_1 and γ_1 states was observed along with another desorption state we label as γ_2 [see Figs. 1(a) and 2(a)]. Based on the correlation to surface oxygen content and the prior observations of Pietsch,[4,46] we attribute the γ_1 and γ_2 states to H_2 and/or H_2O desorption from surface silanol (SiOH) sites. The latter can be detected in our H_2 TPD spectra due to fragmentation of desorbed H_2O in the ionizer of our QMS.[63] As previously described by Pietsch,[46] H_2 and H_2O desorption from surface SiOH sites can occur via the respective reactions: $SiOH + SiOH \rightarrow 2SiO + H_2(g)$, and $SiOH + SiOH \rightarrow Si + SiO + H_2O(g)$. We assign the former to the γ_1 and postulate that the γ_2 may be related to the latter due to the higher temperature and requirement for a Si-O bond to be broken. Further support for this assignment will be provided in Sec. III B covering a detailed kinetic analysis of the TPD spectra shown in Fig. 1.

Examining the TPD spectrum for the Si (001) wafer that was UV/ozone and HF/alcohol spin cleaned *ex-situ* and exposed to the remote H-plasma *in-situ* at 150 °C for 2 min [Fig. 1(b)], one can see that in addition to the β_{1-3} states, more states appear in between the β_1 and β_2 states and at temperatures $> \gamma_2$. The new states in between β_1 and β_2 are attributed to H_2 desorption from subsurface defects, while the higher temperature state at 770 °C (δ_2) is attributed to H_2 evolved during the sublimation of surface oxides (SiO) unintentionally formed during the remote H-plasma processing.[46,64,65] For the former, we note that prior investigations of remote H-plasma cleaned surfaces have shown that low temperature (150 °C) H-plasma exposures can result in the

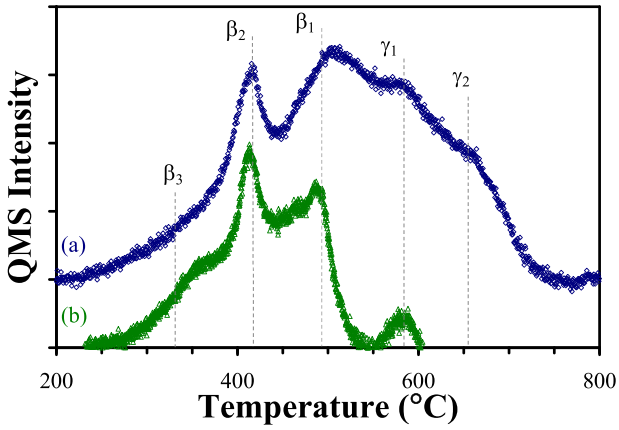

FIG. 2. (Color online) H_2 TPD spectra from Si (001) wafers after *ex-situ* UV/ozone and (a) 10:1 HF dip cleaning with ~0.1 ML O, and (b) HF/alcohol spin cleaning with <0.03 ML O.

formation of subsurface hydrogen-induced platelet defects extending ~25 nm below the plasma treated surface.[66,67] For the latter, we note that AES measurements performed after the remote H-plasma exposure did show a slight increase in surface oxygen content (0.05–0.1 ML) consistent with the possible formation and then sublimation of surface SiO species during the TPD measurement. Some unintentional oxidation of the Si (001) surface during remote H-plasma exposure using a similar experimental setup has been previously reported and attributed to SiO or OH erosion of the quartz tube wall, or contamination produced by the interaction of atomic hydrogen with the chamber walls.[65] Additional support for both of the above assignments will be provided later during the detailed kinetic analysis of these spectra.

When the length of the 150 °C remote H-plasma processing was increased to 60 min [Fig. 1(c)], the newly created desorption states remained but changed slightly in position and intensity. However, the β_3 state completely disappeared, and the LEED pattern post plasma exposure changed from a clear (1×1) to a diffuse (1×1) pattern. The disappearance of the low temperature β_3 state and change in LEED pattern with increased remote H-plasma exposure time at 150 °C suggests that some surface etching and removal of surface SiH_3 groups occurred at 150 °C. This is consistent with prior work by Carter and Montgomery that has shown etching of Si (001) surfaces does indeed occur at these temperatures.[20,21] Using an *in-situ* QMS, they were able to observe the formation of SiH_4 etch products during remote H-plasma exposure via monitoring SiH_2 ($m/e^- = 30$) produced in the QMS ionizer by electron impact ionization. Significant SiH_2 formation was observed when operating the remote H-plasma in the presence of Si at 150 °C, while no SiH_2 was observed when a Si substrate was absent. Significant roughening of the Si (001) surface during remote H-plasma exposure at 150 °C has also been observed by Montgomery using atomic force microscopy (AFM) and is additional evidence of surface etching.[21]

Even more dramatic changes in the H_2 TPD spectra were observed for the Si (001) samples exposed to the remote H-plasma at 450 °C. For a 2 min exposure, the β_2 state completely disappeared and a broad desorption state from 170 to 370 °C appeared that partially overlaps with the β_3 state [see Fig. 1(d)]. Furthermore, a sharp, near exponential increase in H_2 signal started at 700 °C. For the 60 min, 450 °C remote H-plasma exposure, the β_1 state is nearly completely absent and replaced by broad H_2 desorption peaks at 650 and 850 °C [see Fig. 1(e)]. These changes in the H_2 TPD spectra also correspond to changes observed using LEED and AES (see Table I). For LEED, a sharp (2×1) pattern was observed after the 450 °C, 2 min exposure, but no diffraction pattern was observed after the 450 °C, 60 min remote H-plasma exposure. AES measurements performed after the 450 °C, 2 min remote H-plasma treatment showed an increase in oxygen content to 0.1–0.3 ML. However, a dramatic (>10×) increase in surface oxygen content to > 5 ML was observed for the 450 °C, 60 min remote H-plasma exposure. In both cases, a (2×1) LEED pattern was observed after the TPD measurements and AES showed significantly reduced oxygen content (<0.05–0.1 ML) relative to the pre-TPD measurements.

The lack of a β_2 H_2 desorption state and the presence of a (2×1) LEED pattern for the 450 °C, 2 min remote H-plasma exposure TPD spectrum is in agreement with prior studies.[68,69] This indicates the Si surface is primarily terminated with Si-H monohydride species and is consistent with the substrate temperature during plasma processing being slightly above the β_2 dihydride desorption temperature. These observations are also consistent with the QMS studies by Montgomery and Carter where they observed the intensity of the SiH_2 ($m/e^- = 30$) etch product generated during remote H-plasma exposure decreased with decreasing substrate temperature.[20,21] Using AFM, Montgomery additionally observed that remote H-plasma induced surface roughening decreased with decreasing substrate temperatures.[21] At substrate temperatures > 450 °C, no subsurface defects or increase in surface roughness was observed and surface etching observed using the *in-situ* QMS was greatly reduced.

Given the process temperature and lack of a β_2 H_2 desorption state, the lower temperature H_2 desorption feature at 170–370 °C observed for the 450 °C, 2 min sample is surprising. However, this is consistent with H_2 TPD spectra previously acquired from 6H-SiC (0001)–(3×3) surfaces exposed to identical remote H-plasma conditions.[54] In this case, a similar H_2 desorption state was observed from 200 to 500 °C that corresponded with the etching and removal of a Si–Si bilayer residing on the bulk terminated SiC (0001) surface. Based on analogy to the Si (111) surface, the 6H-SiC (0001)–(3×3) H_2 desorption state was attributed to β_3 H_2 and SiH_4 desorption from SiH_3 surface species. As we will discuss further later, we similarly attribute the 170–370 °C H_2 desorption from the 450 °C, 2 min processed Si (001) surface to β_3 H_2 and SiH_4 desorption from SiH_3 surface species. This assignment thus suggests that while surface etching by the remote H-plasma may be greatly reduced at 450 °C, some generation of SiH_3 surface species must still occur (at least initially). This could presumably occur at surface

defects or microfacets created by the *ex-situ* UV ozone and HF clean, or could be facilitated by the presence of surface oxygen that was noticed to increase significantly after the 450 °C remote H-plasma exposure (see Table I). The observation of H_2 desorption at <370 °C despite the 450 °C processing temperature is attributed to the quick ramp down of the sample temperature after the remote H-plasma exposure (>150 °C/min) and the presence during cooling of residual SiH_x etch byproducts and atomic H from the after glow of the remote H-plasma.

As mentioned previously, the higher temperature H_2 desorption features observed at ~650 and 800 °C for the Si (001) surfaces exposed to the remote H-plasma at 150 and 450 °C are attributed to the release of hydrogen during the decomposition and desorption of surface silanol and oxide species. This is based on both the observation of significant oxygen contamination post the remote H-plasma exposure using AES and the prior results of Pietsch where significant H_2 evolution was observed from OH terminated Si surfaces at similar temperatures.[46] Additional support for this assignment will be provided in Sec. III B where we perform a detailed kinetic analysis of all the H_2 TPD spectra in Fig. 1. However, we do note that the significant increase in oxygen observed in AES and oxygen related desorption features in the TPD spectra at 450 °C vs 150 °C suggests that the source of the oxygen contamination during the remote H-plasma exposure is thermally activated. This could possibly be due to greater heating and desorption of H_2O from the surrounding chamber walls or due to increased reactivity of the Si (001) surface with background sources of oxygen.

B. H_2 TPD kinetic analysis

For our kinetic analysis of the H_2 TPD spectra in Fig. 1, we start with the H_2 TPD spectrum for the 450 °C, 2 min remote H-plasma spectrum [Fig. 1(d)]. This is primarily due to the absence in this spectrum of the β_2 H_2 desorption state that overlaps with the β_1 and β_3 states and hence allows a direct analysis of the kinetics of the β_1 state, which has been previously investigated in great detail.[10–19]

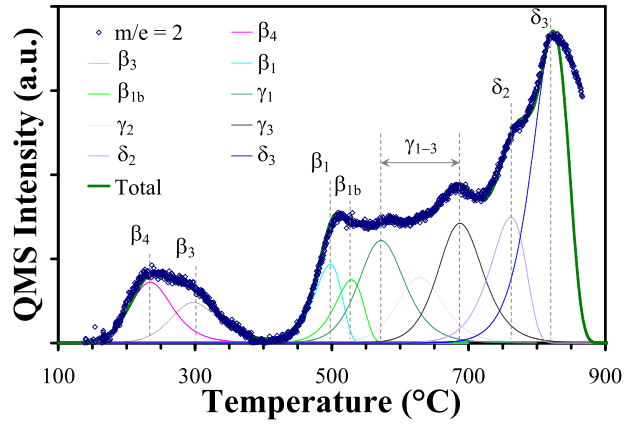

FIG. 4. (Color online) H_2 TPD spectrum from Si (001) wafer exposed to the remote H-plasma at 450 °C for 2 min deconvoluted into various H_2 desorption states.

In Fig. 3, we present a plot of ln (DR) vs 1/T assuming a range of desorption orders and covering the β_1 temperature range for the 450 °C, 2 min remote H-plasma exposed Si (001) wafer. As can be seen, first order desorption kinetics yields a straight line and linear regression analysis indicates $R^2 = 0.99$. This is in excellent agreement with numerous studies of the H_2 desorption kinetics from Si (001) surfaces.[10–14] The activation energy and pre-exponential for desorption determined from the slope and y-intercept of Fig. 3 were $E_d = 2.55 \pm 0.05$ eV and $\nu_1 = 9 \pm 5 \times 10^{14}\,s^{-1}$, respectively. These values are likewise in excellent agreement with the prior literature for the H_2 β_1 desorption state from Si (001) surfaces.[10–14] These kinetic parameters provide an excellent fit to the initial portion of the observed β_1 state, as shown in Fig. 4.

In Fig. 5, we present a similar ln (DR) vs 1/T analysis for the 170–250 °C H_2 desorption observed in Fig. 4. In this case, second order desorption kinetics gave the best linear fit ($R^2 = 0.99$) and the activation energy and pre-exponential for desorption were determined to be $E_d = 1.0 \pm 0.05$ eV and $\nu_2 = 2 \pm 2 \times 10^{-7}$ cm²/s, respectively. As shown in Fig. 4, this well describes the initial portion of the 170–370 °C H_2

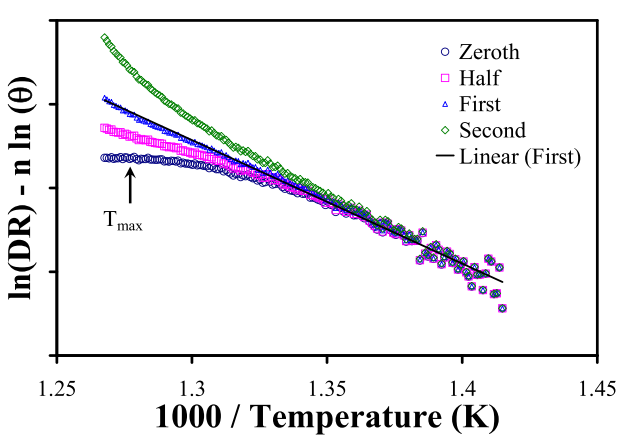

FIG. 3. (Color online) Kinetic analysis described in text for H_2 β_1 peak in Fig. 1(d) for Si (001) exposed to the remote H-plasma at 450 °C for 2 min. Zeroth, half, first, and second order desorption kinetics were considered.

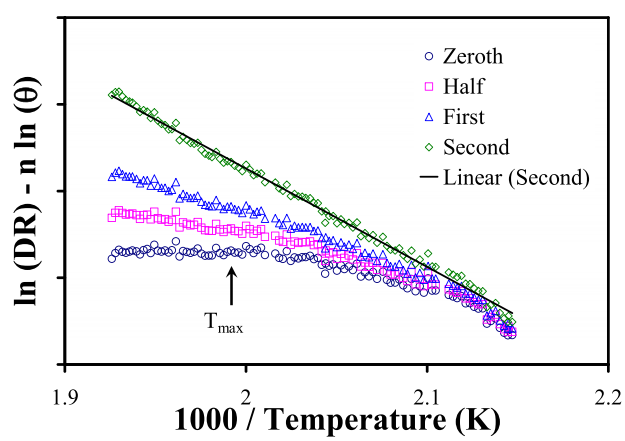

FIG. 5. (Color online) Kinetic analysis described in text for H_2 β_4 peak in Fig. 1(d) for Si (001) exposed to the remote H-plasma at 450 °C for 2 min. Zeroth, half, first, and second order desorption kinetics were considered.

TABLE II. H coverage for various H_2 desorption states shown in Fig. 1 (in ML = 6.78×10^{14} atom/cm^2).

Process	β_4	β_3	β_2	β_{1ss}	β_1	β_{1b}/β_1*	γ_{1-3}	δ_{1-3}	β_4
UV/ozone and HF	—	0.4	0.7	0.3	0.5	0.4	<1.7	—	—
150 °C, 2 min	—	0.5	0.5	0.8	0.7	1.2	—	0.3	—
150 °C, 60 min	—	—	1.0	0.4	0.7	—	2.5	—	—
450 °C, 2 min	0.5	0.4	—	—	0.4	0.4	2.8	3.2	0.5
450 °C, 60 min	—	—	—	—	0.2	0.2	0.9	18	—

desorption, but does not completely reproduce this part of the spectrum.

To completely reproduce the 170–370 °C H_2 desorption window in Fig. 4, we found it necessary to add a second H_2 desorption peak centered at ~310 °C. Due to significant peak overlap, we were not able to perform a similar ln (DR) vs 1/T analysis for this second peak. However, we found that slightly higher, empirically determined values of $E_d = 1.1 \pm 0.05$ eV and $\nu_2 = 3.7 \pm 2 \times 10^{-7}$ cm^2/s allowed the lower temperature portion of Fig. 4 to be well reproduced. Due to the close correspondence in peak temperature and E_d, we label this higher temperature state β_3 and the lower peak temperature state β_4. The E_d for both states is only slightly reduced relative to the value of 1.35 ± 0.09 eV previously determined by Greenlief *et al.* for first order decomposition of surface SiD_3 species using combined TPD and temperature programmed static secondary ion mass spectrometry measurements.[69] In this case, we note that first order kinetics were assumed in the Greenlief analysis rather than deduced. We also note that the β_3 H_2 desorption state has been previously correlated with simultaneous SiH_4 desorption from SiH_3 surface states.[10,15]

The above analysis clearly supports our initial assignment of the 170–370 °C H_2 TPD spectrum to H_2 desorption from SiH_3 related surface species. It also supports our assertion that while surface etching by the remote H-plasma may be greatly reduced at 450 °C, some generation of SiH_3 surface species that are precursors to the SiH_4 etch product must still occur. As for the origin of the β_4 vs β_3 states, we postulate that the former may be due to SiH_3 species originating from surface defects, roughness, or contamination and the latter due to SiH_3 species originating from (001) terraces. We also note the possibility that the β_4 state may be due to desorption of H_2O adsorbed during cool down. This would be consistent with the β_4 state not being observed in the 150 °C remote H-plasma TPD spectra where less heating of the internal remote H-plasma chamber surfaces occurred. The temperature range for the β_4 state is also consistent with that for H_2 observed during H_2O desorption from other surfaces.[63,71,72] However, the activation energy deduced for the β_4 is two times that for H_2O desorption.[63]

As shown in Fig. 4, an additional β_{1b} state and several other peaks previously assigned to H_2 desorption from surface silanols (γ_{1-3}) and H_2 evolved during SiO desorption ($\delta_{2,3}$) were required to reasonably reproduce the higher temperature portion of the TPD spectrum for the 450 °C, 2 min remote H-plasma sample. However, independent analysis of the kinetics for each of these peaks was not possible due to the significant overlap of these desorption states in this spectrum. In order to support the kinetic parameters utilized to fit the remaining portions of the TPD spectrum in Fig. 4 (summarized in Tables II and III), we rely on kinetic analysis of the other TPD spectra in Fig. 1 where some of these states are absent and/or more isolated from the others.

In this regard, we next examine the TPD spectrum for the 150 °C, 60 min remote H-plasma Si (001) wafer where the β_4 and β_3 states are absent and hence direct analysis of the observed β_2 state is possible. Figure 6 presents the ln (DR) vs 1/T analysis for the β_2 peak in this spectrum where second order kinetics provided the best linear fit ($R^2 = 0.99$). The activation energy and pre-exponential for desorption were determined to be $E_d = 2.8 \pm 0.05$ eV and $\nu_2 = 3 \pm 2 \times 10^4$ cm^2/s, respectively. As shown in Fig. 7, these parameters provide an excellent fit to the β_2 peak for the 150 °C, 60 min remote H-plasma spectrum.

TABLE III. Peak desorption temperatures, activation energies, and pre-exponentials for H_2 desorption from Si (001) surfaces investigated in this study. Note: the error bars represent the range of values determined for each state from all the presented TPD spectra.

State	Assignment	Order	T_{max} (°C)	E_d (eV)	ν_d (ν_2 cm^2/s) (ν_1 s^{-1})
β_4	SiH_3	Second	235 ± 5	1.0 ± 0.05[a]	$2 \pm 2 \times 10^{-7}$
β_3	SiH_3	Second	330 ± 20	1.25 ± 0.15[b]	$1 \times 10^{-6\pm1}$
β_2	SiH_2	Second	410 ± 10	2.8 ± 0.05[a]	$3 \times 10^{4.5\pm0.5}$
β_{1ss}	Subsurface defects	First	480 ± 5	2.35 ± 0.05[b]	$9 \pm 1 \times 10^{14}$
β_1	SiH	First	510 ± 5	2.5 ± 0.05[a]	$9 \pm 1 \times 10^{14}$
β_{1b}	SiH	First	540 ± 10	2.6 ± 0.05[b]	$9 \pm 1 \times 10^{14}$
β_1*	SiH from (111) facets	Second	555 ± 5	3.6 ± 0.05[a]	$4 \pm 4 \times 10^5$
γ_1	SiOH	Second	575 ± 5	2.55 ± 0.05[a]	$1 \times 10^{-1\pm1}$
γ_2	SiOH	Second	650 ± 5	2.95 ± 0.05[b]	1 ± 1
γ_3	SiOH	Second	720 ± 10	3.45 ± 0.05[a]	40 ± 10
δ_1	SiO from SiO_2/Si interface	Second	660 ± 5	2.2 ± 0.05[a]	$2 \pm 2 \times 10^{-5}$
δ_2	SiO from SiO_2	First	760 ± 10	3.5 ± 0.05[a]	$3 \pm 3 \times 10^{15}$
δ_3	SiO from SiO_2	First	820 ± 10	3.9 ± 0.05[b]	$2 \pm 2 \times 10^{16}$

[a]E_d determined by ln (DR) vs 1/T analysis.
[b]E_d determined via fitting of TPD spectrum.

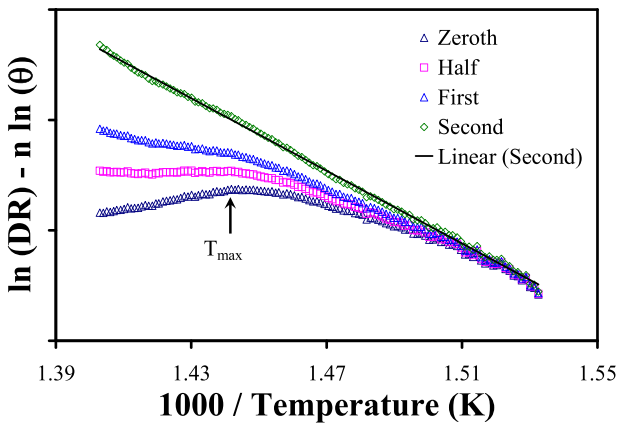

FIG. 6. (Color online) Kinetic analysis described in text for H_2 β_2 peak in Fig. 1(c) for Si (001) exposed to the remote H-plasma at 150 °C for 60 min. Zeroth, half, first, and second order desorption kinetics were considered.

The observation of second order kinetics for the β_2 state is consistent with the kinetic analysis by Gupta[70] of H_2 desorption from porous Si observed using Fourier-transform infrared spectroscopy, and by Flowers of the β_2 state in TPD spectra from both Si (001) and (111) surfaces.[13,16] However, the activation energy for desorption of 2.8 eV determined for the β_2 state here is substantially larger than the value of 1.86 eV determined by Gupta and utilized in the Flowers analysis. In this regard, we note that we were not able to obtain a satisfactory fit to the β_2 state in this study using the Gupta and Flowers desorption parameters. We also note that in both the Gupta and Flowers studies, the ratio of Si-H to Si-H_2 species was roughly 3:1, whereas in our study, the ratio is closer to 1:1. The higher concentration of Si-H_2 species may be responsible for the observed higher β_2 E_d and suggests a surface coverage dependence for the E_d of this state.

As shown in Fig. 7, we found it necessary to incorporate two β_1 desorption states in order to reasonably reproduce the H_2 TPD spectrum above the β_2 desorption state. In this case, we utilized the pre-exponential and activation energy previously determined from Fig. 3 for the higher temperature β_1 state and the same pre-exponential, but a slightly lower

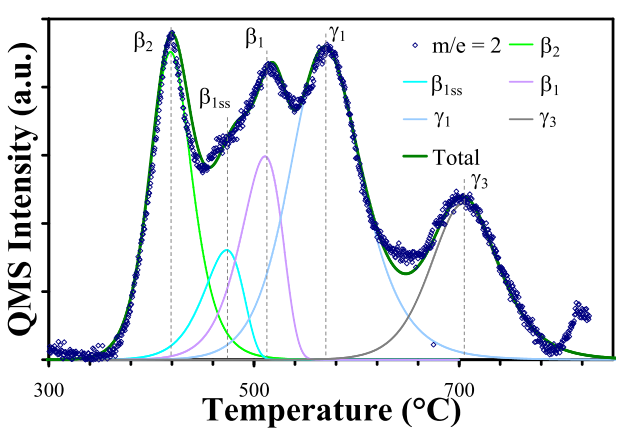

FIG. 7. (Color online) H_2 TPD spectrum from Si (001) wafer exposed to the remote H-plasma at 150 °C for 60 min deconvoluted into various H_2 desorption states.

activation energy of 2.4 eV for the lower temperature β_{1ss} state. The lower temperature β_{1ss} state is attributed to H_2 evolution/desorption from the previously mentioned subsurface defects created by the remote H-plasma exposure. The slightly lower desorption temperature and activation energy is consistent with prior observations by Hess and Kim of H_2 desorption from subsurface B-H complexes and/or H-Si_2B surface species.[36,37] At this point, it is also worth briefly discussing the higher E_d determined for the β_2 state relative to the β_1 state even though the β_2 state has a lower peak desorption temperature. This is attributed to the difference in the desorption order for the two states. As shown by Schulze, the activation energy for the β_1 state would be substantially higher (3.5 eV) if second order kinetics were assumed.[15]

To completely reproduce the H_2 TPD spectrum shown in Fig. 7, two additional higher temperature desorption peaks (γ_1 and γ_3) centered at ~570 and 700 °C were required. The ln (DR) vs 1/T analysis for both peaks (not shown) indicated second order desorption kinetics in both cases. For the γ_1 state at 570 °C, the activation energy and pre-exponential for desorption were determined to be 2.45 ± 0.05 eV and $1 \pm 1 \times 10^{-2}$ cm^2/s, respectively. For the γ_3 state, $E_d = 3.5 \pm 0.05$ eV and $\nu_2 = 50 \pm 50$ cm^2/s were determined. Using these parameters, the H_2 TPD spectrum for the 150 °C, 60 min remote H-plasma exposed Si (001) surface can be reasonably reproduced (see Fig. 7).

The desorption activation energy determined for the γ_1 state is in excellent agreement with the value of 2.4 eV previously determined for H_2 desorption from isolated surface hydroxide species on dilute HF treated AlN surfaces.[63] The γ_1 desorption activation energy is also in approximate agreement with the value of 2.1 eV previously determined by Proost for the desorption of H_2O from isolated silanol groups in spin on silicate glass films.[71,72] In this regard, we do note that the γ_1 state could represent primarily H_2O desorption since H_2 ($m/e^- = 2$) can be produced by electron impact fragmentation of H_2O in the ionizer of our QMS.[63] However, either interpretation supports our assignment of the γ_1 state to surface silanol groups.

The desorption activation energy determined for the γ_3 state is in reasonable agreement with the value of 3.2 eV previously determined for H_2 evolved during the desorption of surface oxides from AlN surfaces treated in dilute HF solutions. It is also in excellent agreement with the values of 3.0–4.0 eV reported for SiO desorption from oxidized Si (001) and (111) surfaces.[73–80] For the latter, first order kinetics have been primarily reported whereas second order kinetics have been determined here for the γ_3 state. This suggests the γ_3 state represents the recombination of two surface SiOH species resulting in simultaneous SiO and H_2 desorption via the following reaction: $2\ SiOH \rightarrow 2\ SiO(v) + H_2(g)$.

In Fig. 8, we present the TPD spectrum acquired from the Si (001) wafer exposed to the remote H-plasma at 150 °C for 2 min decomposed into various desorption states. To reproduce the portion of the TPD spectrum below the labeled β_1 state, we largely utilized the desorption kinetics previously determined for the β_{1-3} states. For the lowest temperature portion of the spectrum, we found that the β_3 activation

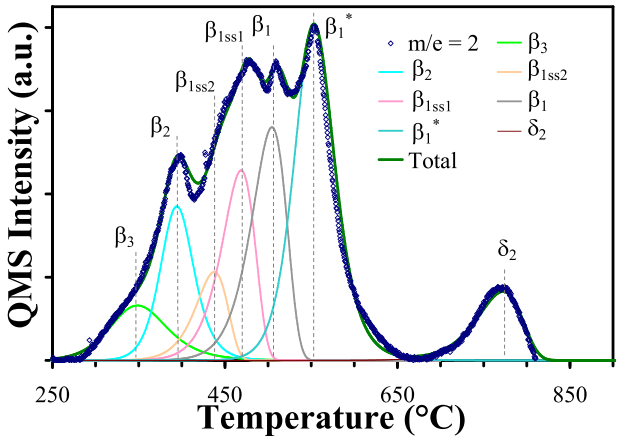

FIG. 8. (Color online) H_2 TPD spectrum from Si (001) wafer exposed to the remote H-plasma at 150 °C for 2 min deconvoluted into various H_2 desorption states.

energy of 1.35 eV determined by Greenlief[69] provided a more visibly satisfying reproduction of the lower temperature portion of the spectrum in conjunction with the parameters determined in this study for the β_2 state. For the portion of the TPD spectrum between the β_2 and β_1 states, we found it necessary to utilize three β_1 states with identical pre-exponentials but increasing activation energies of 2.3, 2.4, and 2.5 eV. As for the 150 °C, 60 min spectrum, we attribute the lower temperature β_{1ss} states to H_2 desorption from subsurface defects states.

Slightly above the highest temperature β_1 state lies a second H_2 desorption state at 550 °C that we have labeled the β_1* state. Based on prior assignments and the peak temperature of the β_1* state, it is tempting to attribute it to the γ_1 state. However, the ln (DR) vs 1/T analysis of this peak indicates second order desorption kinetics with a completely different desorption activation energy and pre-exponential of 3.6 eV and 4×10^5 cm^2/s, respectively. In conjunction with the parameters utilized for the other β_{1-3} states, the derived β_1* parameters provide an excellent reproduction of the lower temperature portion of the TPD spectrum in Fig. 8.

Due to the known surface etching that occurs at this temperature by the remote H-plasma, one possibility is that the β_1* state represents H_2 desorption from monohydride surface species present on (111) facets created during the remote H-plasma exposure. H_2 desorption from Si (111) surfaces has generally been reported to occur at a slightly higher temperature relative to the (001) surface and second order H_2 desorption kinetics from Si (111) surface have been consistently reported.[54] Unfortunately, the activation energy determined for the observed β_1* state is substantially higher than the values of 2.5–2.7 eV typically reported for monohydride desorption from Si (111) surfaces. In this regard, we do note that the previously reported activation energies for monohydride desorption from Si (111) do provide an approximate fit to the β_1* state in Fig. 8. This suggests that there is some relation between the observed β_1* state and the Si (111) β_1 state with the higher activation energy for the β_1* state possibly representing some other intermediary surface facet created by remote H-plasma etching of the Si (001) surface.

Another possibility is the β_1* state is related to a β_{1b} state previously observed by Narita and attributed to H_2 desorption from SOD.[33] As previously discussed, Narita has shown that for Si (001) surfaces the β_1 state is actually composed of two peaks: a lower temperature β_{1a} peak attributed to H_2 desorption from DOD and a higher temperature β_{1b} peak attributed to H_2 desorption from SOD.[33–35] The lower temperature β_{1a} state exhibits first order kinetics while the higher temperature β_{1b} state exhibits second order kinetics. This is consistent with our observations for the β_1 and β_1* state. However, the β_{1b} E_d of 2.15 ± 0.27 eV determined by Namiki for 1 ML coverage is substantially smaller than the value determined here.[33]

Above the β_1* state in Fig. 8, another H_2 desorption state was observed at ~770 °C that we have labeled δ_2 and attributed to H_2 evolved during desorption of surface SiO species. The ln (DR) vs 1/T analysis presented in this case indicates first order kinetics with an activation energy and pre-exponential of 3.55 ± 0.05 eV and $3 \pm 3 \times 10^{15}$ s^{-1}, respectively. As shown in Fig. 8, these parameters provide an excellent reproduction of the δ_2 state and the remaining 150 °C, 2 min TPD spectrum.

We next examine the various desorption states that comprise the H_2 TPD spectrum acquired from the 450 °C, 60 min remote H-plasma Si (001) surface. We first note the lack in Fig. 9 of any β_{1ss} desorption states attributed to subsurface defect states. This is consistent with the TPD spectrum in Fig. 4 for the 450 °C, 2 min remote H-plasma treated surface and prior TEM investigations that have shown the absence of such defects for 450 °C remote H-plasma treated Si (001) surfaces.[21]

As shown in Fig. 9, the parameters previously determined for the β_1 state reasonably reproduced the initial small rise in H_2 desorption starting at ~450 °C. In this case, two β_1 states were again needed to reproduce this portion of the TPD spectrum, but with the higher temperature state having a slightly higher activation energy of 2.65 eV. A similar higher temperature β_1 state was also observed in the 450 °C, 2 min remote H-plasma TPD spectrum (see Fig. 4). Due to the lower E_d and closer correspondence with the results of Namiki,[33] we have labeled these two higher temperature β_1 states β_{1b}. However, we do note that Namiki determined second order kinetics for the β_{1b} state whereas we found first order kinetics for β_{1b} allowed the H_2 TPD spectra in Figs. 4 and 9 to be better reproduced. We also note that due to identical peak temperatures (~550 °C), it is possible that the β_{1b} and previously discussed β_1* state are related.

Above the β_1 states in Fig. 9, a broad H_2 desorption peak ranging from ~550 to 700 °C can be clearly identified that we have labeled the δ_1 state. The ln (DR) vs 1/T analysis of this feature clearly indicates second order kinetics with a desorption activation energy and pre-exponential of 2.2 eV and 2×10^{-5} cm^2/s, respectively. This activation energy is extremely low relative to the values previously determined for lower temperature desorption states. However, as we will show, this value is consistent with prior investigations of the

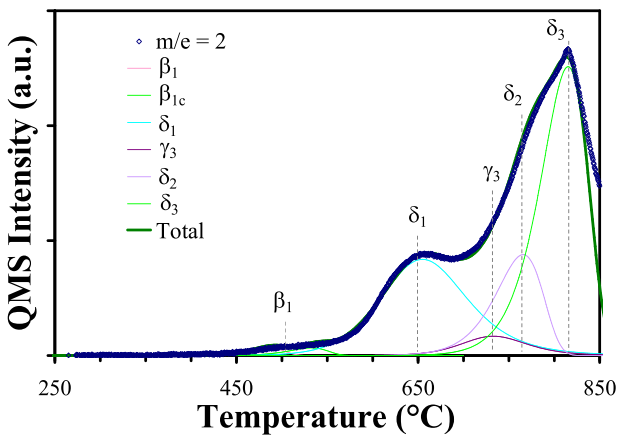

FIG. 9. (Color online) H_2 TPD spectrum from Si (001) wafer exposed to the remote H-plasma at 450 °C for 60 min deconvoluted into various H_2 desorption states.

kinetics of oxide decomposition and SiO desorption from Si surfaces.

To complete the fitting of Fig. 9 beyond the δ_1 state, we found it necessary to add higher temperature γ_3, δ_2, and δ_3 states at ~730, 755, and 815 °C. For the γ_3 and δ_2 states, we utilized the parameters previously determined from the 150 °C, 60 min, and 150 °C, 2 min spectra, respectively. The parameters for the δ_3 states were drawn from literature reported values for the kinetics of surface oxide decomposition and SiO desorption from Si and other surfaces[73–79] and then empirically adjusted slightly to improve the visible quality of fit. The optimum desorption activation energy and pre-exponential values for the δ_3 state were determined to be $E_d = 3.9 \pm 0.05$ eV and $\nu_1 = 2 \times 10^{16}\,s^{-1}$, respectively. Using these parameters and the H coverage summarized in Table III, the 450 °C, 60 min remote H-plasma TPD spectrum was adequately reproduced.

Support for the kinetic parameters determined for the δ_{1-3} states and the assignment to H_2 evolved during desorption of SiO species can be gained by examining prior investigations of surface oxide desorption from Si (001) surfaces. As mentioned previously, Pietsch has shown that oxidized hydrophilic Si (111) surfaces prepared using an *ex-situ* NH_4OH:H_2O_2:H_2O clean exhibit a rapid increase in H_2 desorption starting at ~900 °C that corresponds with a similar increase in SiO partial pressure.[46] Based on this correspondence, Pietsch attributed the observed H_2 signal to hydrogen liberated during the decomposition and sublimation of the oxide as SiO via the reaction $Si + SiO_2 \rightarrow SiO$. A more detailed study by Kobayashi *et al.* of the desorption of surface oxides formed via various *ex-situ* treatments of Si (111) surfaces has shown that SiO desorption can occur from 750 to 950 °C with the peak desorption temperature increasing with increasing surface oxide thickness.[73] These results are consistent with the 450 °C, 60 min remote H-plasma TPD spectrum where an exponential increase in evolved H_2 was observed starting at ~700 °C and a significant decrease in surface oxygen content after TPD was observed using AES.

More detailed modulated beam experimental investigations of the kinetics of SiO desorption from Si (111) and (001) surfaces have largely reported first order desorption kinetics, which is also consistent with the kinetics determined for the δ_2 and δ_3 states observed in this study. However, the reported SiO desorption activation energies have a bimodal distribution ranging from 2.4 to 2.8 (Ref. 74) and 3.0 to 4.0 eV,[75–77] while theoretical investigations have largely pointed to higher desorption energies of 3.4–4.2 eV.[78–80] The range in experimentally reported SiO desorption activation energies can be understood based on several additional studies of the thermal decomposition of SiO_2 on Si (001) surfaces that have shown the process is not spatially homogeneous. Specifically, several scanning Auger and electron microscopy studies have shown that decomposition of native (0.3 nm) and thin (5–50 nm) oxide films on Si (001) occurs locally at the vacuum/SiO_2/Si linear interface.[81–83] The activation energy for the progression of this linear boundary has been reported to be ~2.0 eV and it has been suggested that the activation energy for the $Si + SiO_2 \rightarrow SiO$ reaction is 4.0 eV.[83] This has been supported by detailed TPD measurements performed by Sun that have shown SiO desorption from a continuous (4.5 ML) oxide on Si (001) occurs with a peak temperature of ~875 °C, while desorption of SiO from the clean Si (001) surface ($\ll$ 1 ML O) occurs at a lower temperature of ~720 °C.[84] For the higher temperature desorption peak, Sun determined first order kinetics with an activation energy of 3.9 eV in agreement with the higher activation energies previously determined using modulated molecular beam techniques and our results for the δ_3 state.[75–77] While Sun did not determine the desorption kinetics for the lower temperature TPD peak, it can be safely assumed that the activation energy would be significantly lower and, based on the peak temperature of ~720 °C, closer to the values of 3.0–3.4 eV for the $\gamma_{1,2}$ and δ_2 states that were observed at similar temperatures in this study. These numbers would also be consistent with the lower range of values reported for SiO desorption in the literature. Based on the similarities in activation energies (2.0 vs 2.2 eV), it seems reasonable to attribute the δ_1 state to SiO desorption from the vacuum/SiO_2/Si interface.[74,81–83]

The significant amount of hydrogen released during desorption of surface oxides from Si (001) suggests that hydrogen plays a role in the desorption mechanism. In this regard, we propose for the δ_1 state that SiO desorption occurs via a reaction such as $Si–Si + HOSiO \rightarrow Si + H_2 + SiO(v) + SiO$. This reaction would be consistent with the second order kinetics observed in this study for the δ_1 state and prior observations that surface oxide decomposition occurs at the vacuum/SiO_2/Si interface. For the $\delta_{2,3}$ states where first order kinetics have been observed, we postulate that H_2 and SiO are liberated simultaneously through direct reaction of surface silanols similar to that proposed for the γ_3 state [i.e., $2SiOH \rightarrow 2SiO(v) + H_2(g)$]. The primary difference between the two mechanisms is that γ_3 involves isolated silanols ($\theta < 1$ ML) and is second order whereas $\delta_{2,3}$ involves adjacent/pre-paired silanols ($\theta < 1$ ML) and is first order.

Finally in Fig. 10, we illustrate that the TPD spectrum from the *ex-situ* UV/ozone and 10:1 HF dip cleaned Si (001)

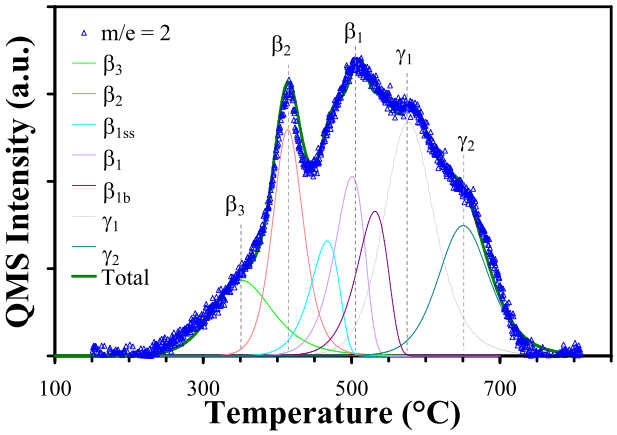

FIG. 10. (Color online) H_2 TPD spectrum from Si (001) with only the *ex-situ* UV/ozone and 10:1 HF dip clean deconvoluted into various H_2 desorption states.

surface can be well reproduced using the kinetic parameters determined for the β_{1-3} and γ_{1-2} states from the previously examined remote H-plasma TDP spectra. As for the 150 °C remote plasma spectra, we found it necessary to incorporate three β_1 states to completely fit the regions between the β_2 and β_1 states. In this case, we attribute the lower temperature β_{1ss} state to desorption of hydrogen dissolved in the substrate during the aqueous HF treatment, and the higher temperature β_{1b} state to H_2 desorption from lower index planes that may have formed due to slight surface etching by the aqueous HF treatment and/or β_1 desorption from SOD.[33] Evidence for the former has been previously demonstrated by Thanh.[48]

For the UV/ozone and HF TPD spectrum, the observation of only $\gamma_{1,2}$ states attributed to OH species and the lack of δ_{1-3} states attributed to surface oxides (SiO_2) and SiO desorption is consistent with the high SiO_2 etch rate for aqueous HF solutions and previous demonstrations of the resistance of HF processed Si surfaces to oxidation during subsequent air exposure.[45,46] However, based on the TPD measurements performed by Tomita[61] and Kinoshita[62] on aqueous HF processed Si (001) surfaces, it is possible that the γ_1 state in Fig. 10 may also be related to some desorption of fluorinated species such as F_2, SiF_x, or SiH_3F. Both authors have reported observing desorption of such fluorinated species at temperatures of ~600 °C, which is in the approximate range of the γ_1 state. However, due to the high reactivity of atomic hydrogen with fluorine, it is extremely unlikely that the γ_1 state observed in the remote H-plasma treated TPD spectra is related to desorption of fluorine related species.[25,85] Also, the activation energy of 3.7 eV for SiF_2 desorption from Si (001) reported by Engstrom[86] is substantially higher than the values determined for the γ_1 and γ_2 states.

As some carbon contamination was noticed using AES for all Si (001) surfaces investigated in this study, it is worth also discussing the assignment of the γ_{1-3} and other states with respect to H_2 desorption from carbon related surface species. As mentioned previously, Pietsch[46] and Kawase[60] have observed and attributed a broad H_2 and CH_4 desorption peak from 300 to 700 °C (peaking at ≅450 °C) to residual organic surface contaminants after *ex-situ* aqueous HF processing. This desorption state is too broad and at too low a temperature to be attributed directly to any of the observed states. As the carbon contamination was <0.02 ML, any H_2 desorption from such states would likely only contribute to the background H_2 TPD signal.

In Table II, we have summarized the H coverage determined for all of the various individual β states observed as well as the sum coverage for the γ and δ states. Excluding the results from the 450 °C, 60 min sample that are mostly related to H_2 evolved from unintentionally formed surface oxides, the H_2 evolved from all the β states ranges from 2.1 to 3.8 ML. Counting just the H_2 evolved from surface β sites, the total H_2 surface coverage ranges from 1.7 to 2.2 ML, which is in excellent agreement with the saturation surface coverage of 1.8–2.0 ML previously determined by Oura[87] and Hess[39] for Si (001). This indicates that approximately 1–2 ML of hydrogen is located below the outer most Si surface in hydrogen generated defects.

Regarding the H_2 evolved from the γ and δ states, the H_2 coverage tracks with the amount of oxygen detected pre-TPD using AES. However, the TPD H_2 coverage exceeds the AES O coverage in some cases by 2–10×. Some of this is likely due to experimental errors and differences in surface coverage calibration and calculation for TPD (H) and AES (O). For AES, in particular, the surface coverage calculation assumed a continuous layer/film. However, if the surface oxide formed as islands or a discontinuous film, this could result in a significant underestimation of the oxygen surface coverage. It is also possible for a significant amount of hydrogen to reside in a SiO_2 island or film as SiOH. Both of these observations would explain why the amount of H_2 evolved from the γ and δ states exceeded that from the β_1 state for the Si (001) surfaces exposed to 450 °C remote H-plasma. Lastly, it is also possible for a significant amount of hydrogen to reside at the Si/SiO_2 interface. It is well known that due to a lack of complete epitaxial registry between Si and SiO_2, a significant concentration of interfacial silicon dangling bonds exists that could be terminated by hydrogen.[88] The presence of such interfacial Si-H species could allow the β_{1-3} coverage to still approach or exceed 1 ML even with an overlying surface oxide.

IV. SUMMARY AND CONCLUSIONS

In summary, TPD has been utilized to examine both the range of hydrogen related surface species formed on Si (001) by *ex-situ* aqueous HF and *in-situ* remote H-plasma treatments and the associated H_2 desorption kinetics from these surfaces. A wide range of H_2 desorption states were observed and attributed to surface mono/di/trihydrides, hydroxides, oxides, and subsurface defects. For Si (001) surfaces exposed to a remote H-plasma at 150 °C, H_2 desorption from a mix of surface mono/di/trihydrides and subsurface states was observed. Remote H-plasma exposures at temperatures of 450 °C were instead observed to result in H_2 desorption from primarily monohydride surface states and unintentionally formed silanol and surface oxides. The

kinetics for H_2 desorption from all these states were found to be in excellent agreement with those previously determined for Si (001) and (111) exposed to O_2 and thermally generated sources of H under pure UHV conditions.

ACKNOWLEDGMENTS

This work was supported by the ONR under Contract Nos. N00014-91-J-1410 and N00014-92-J1477, and by the Department of Education through an Electronic Materials Fellowship.

[1]M. Greenlief and M. Armstrong, J. Vac. Sci. Technol., B **13**, 1810 (1995).
[2]B. Deal and A. Grove, J. Appl. Phys. **36**, 3770 (1965).
[3]C. Cardinaud, M. Peignon, and P. Tessier, Appl. Surf. Sci. **164**, 72 (2000).
[4]G. Pietsch, Appl. Phys. A **60**, 347 (1995).
[5]B. Anthony, L. Breaux, T. Hsu, S. Banerjee, and A. Tasch, J. Vac. Sci. Technol., B **7**, 621 (1989).
[6]G. Pietsch, Y. Chabal, and G. Higashi, Surf. Sci. **331**, 395 (1995).
[7]E. Cartier, J. Stathis, and D. Buchanan, Appl. Phys. Lett. **63**, 1510 (1993).
[8]J. Sullivan, W. Graham, R. Tung, and F. Schrey, Appl. Phys. Lett. **62**, 2804 (1993).
[9]A. Urbanowicz, K. Vanstreels, D. Shamiryan, S. De Gendt, and M. Baklanov, Electrochem. Solid-State Lett. **12**, H292 (2009).
[10]S. Gates, R. Kunz, and C. Greenlief, Surf. Sci. **207**, 364 (1989).
[11]K. Sinniah, M. Sherman, L. Lewis, W. Weinberg, J. Yates, Jr., and K. Janda, Phys. Rev. Lett. **62**, 567 (1989).
[12]U. Hofer, L. Li, and T. Heinz, Phys. Rev. B **45**, 9485 (1992).
[13]M. Flowers, N. Jonathan, Y. Liu, and A. Morris, J. Chem. Phys. **99**, 7038 (1993).
[14]D. Lin and R. Chen, Phys. Rev. B **60**, R8461 (1999).
[15]G. Schulze and M. Henzler, Surf. Sci. **124**, 336 (1983).
[16]M. Flowers, N. Jonathan, A. Morris, and S. Wright, J. Chem. Phys. **108**, 3342 (1998).
[17]M. Wise, B. Koehler, P. Gupta, P. Coon, and S. George, Surf. Sci. **258**, 166 (1991).
[18]G. Reider, U. Hofer, and T. Heinz, J. Chem. Phys. **94**, 4080 (1991).
[19]A. Namiki, Prog. Surf. Sci. **81**, 337 (2006).
[20]R. Carter, T. Schneider, J. Montgomery, and R. Nemanich, J. Electrochem. Soc. **141**, 3136 (1994).
[21]J. Montgomery, T. Schneider, R. Carter, J. Barnak, Y. Chen, J. Hauser, and R. Nemanich, Appl. Phys. Lett. **67**, 2194 (1995).
[22]J. Vander Weide and R. Nemanich, Appl. Phys. Lett. **62**, 1878 (1993).
[23]B. Coppa, C. Fulton, S. Kiesel, R. Davis, C. Pandarinath, J. Burnette, R. Nemanich, and D. Smith, J. Appl. Phys. **97**, 103517 (2005).
[24]B. Thedjoisworo, D. Cheung, and D. Zamani, J. Vac. Sci. Technol., A **30**, 031303 (2012).
[25]H. Seo, B. Kim, J. Song, Y. Kim, H. Soh, Y. Kim, and H. Jeon, J. Vac. Sci. Technol., B **20**, 1548 (2002).
[26]M. Baklanov, D. Shamiryan, Zs. Tokei, G. Beyer, T. Conard, S. Vanhaelemeersch, and K. Maex, J. Vac. Sci. Technol., B **19**, 1201 (2001).
[27]X. Liu, S. Gill, F. Tang, S. King, and R. Nemanich, J. Vac. Sci. Technol., B **30**, 031212 (2012).
[28]J. Boland, Phys. Rev. Lett. **65**, 3325 (1990).
[29]C. Cheng and J. Yates, Jr., Phys. Rev. B **43**, 4041 (1991).
[30]Z. Lu, K. Griffiths, P. Norton, and T. Sham, Phys. Rev. Lett. **68**, 1343 (1992).
[31]C. M. Greenlief and M. Liehr, Appl. Phys. Lett. **64**, 601 (1994).
[32]C. Kleint and K. Brzoska, Surf. Sci. **231**, 177 (1990).
[33]Y. Narita, Y. Kihara, S. Inanaga, and A. Namiki, Surf. Sci. **603**, 1168 (2009).
[34]Y. Narita, S. Inanaga, C. Unoko, and A. Namiki, Surf. Sci. **605**, 32 (2011).
[35]Y. Narita, S. Inanaga, and A. Namiki, J. Appl. Phys. **113**, 234309 (2013).
[36]G. Hess, *et al.*, Appl. Phys. Lett. **71**, 2184 (1997).
[37]H. Kim, G. Glass, S. Park, T. Spila, N. Taylor, J. Abelson, and J. Greene, Appl. Phys. Lett. **69**, 3869 (1996).
[38]Y. Foo, K. Bratland, B. Cho, J. Soares, P. Desjardins, and J. Greene, Surf. Sci. **513**, 475 (2002).
[39]G. Hess, M. Russell, B. Gong, P. Parkinson, and J. Ekerdt, J. Vac. Sci. Technol., A **15**, 1129 (1997).
[40]C. Herrero, M. Stutzman, A. Breitschwerdt, and P. Santos, Phys. Rev. B **41**, 1054 (1990).
[41]W. Beyer and H. Wagner, J. Appl. Phys. **53**, 8745 (1982).
[42]W. Zongyan, B. Equer, A. Lloret, and R. Amokrane, Physica B **170**, 523 (1991).
[43]M. Grundner and H. Jacob, Appl. Phys. A **39**, 73 (1986).
[44]D. Graf, M. Grundner, and R. Schulz, J. Vac. Sci. Technol., A **7**, 808 (1989).
[45]Y. Chabal, G. Higashi, K. Raghavachari, and V. Burrows, J. Vac. Sci. Technol., A **7**, 2104 (1989).
[46]G. Pietsch, U. Kohler, and M. Henzler, J. Vac. Sci. Technol., B **12**, 78 (1994).
[47]N. Hirashita, M. Kinoshita, I. Aikawa, and T. Ajioka, Appl. Phys. Lett. **56**, 451 (1990).
[48]V. Thanh, D. Bouchier, and G. Hincelin, J. Appl. Phys. **87**, 3700 (2000).
[49]S. King, R. Nemanich, and R. Davis, J. Electrochem. Soc. **146**, 1910 (1999).
[50]S. King, R. Nemanich, and R. Davis, J. Electrochem. Soc. **146**, 2648 (1999).
[51]S. King, C. Ronning, R. Davis, R. Busby, and R. Nemanich, J. Appl. Phys. **84**, 6042 (1998).
[52]D. Fenner, D. Biegelsen, and R. Bringans, J. Appl. Phys. **66**, 419 (1989).
[53]S. King, R. Nemanich, and R. Davis, Surf. Sci. **602**, 405 (2008).
[54]S. King, R. Davis, and R. Nemanich, Surf. Sci. **603**, 3104 (2009).
[55]R. Culbertson, L. Feldman, and P. Silverman, J. Vac. Sci. Technol. **20**, 868 (1982).
[56]J. Craig, Jr., C. Cariss, and M. Craig, J. Vac. Sci. Technol., A **11**, 554 (1993).
[57]J. Miller, H. Siddiqui, S. Gates, J. Russell, Jr., J. Yates, Jr., J. Tully, and M. Cardillo, J. Chem. Phys. **87**, 6725 (1987).
[58]D. Parker, M. Jones, and B. Koel, Surf. Sci. **233**, 65 (1990).
[59]B. Doris, J. Fretwell, J. Erskine, and S. Banerjee, Appl. Phys. Lett. **70**, 2819 (1997).
[60]K. Kawase, J. Tanimura, H. Kurokawa, K. Wakao, M. Inoue, H. Umeda, and A. Teramoto, J. Electrochem. Soc. **152**, G163 (2005).
[61]H. Tomita, T. Kikuchi, and K. Furuya, Jpn. J. Appl. Phys., Part 1 **30**, 897 (1991).
[62]K. Kinoshita and I. Nishiyama, J. Vac. Sci. Technol., A **13**, 2709 (1995).
[63]S. King, R. Davis, and R. Nemanich, J. Vac. Sci. Technol., A **32**, 051402 (2014).
[64]R. Thomas, M. Mantini, R. Rudder, D. Malta, S. Hattangady, and R. Markunas, J. Vac. Sci. Technol., A **10**, 817 (1992).
[65]B. Anthony, T. Hsu, L. Breaux, R. Qian, S. Banerjee, and A. Tasch, J. Electron. Mater. **19**, 1027 (1990).
[66]N. Johnson, F. Ponce, R. Street, and R. Nemanich, Phys. Rev. B **35**, 4166 (1987).
[67]T. Hsu, B. Anthony, R. Qian, J. Irby, S. Banerjee, A. Tasch, S. Lin, H. Marcus, and C. Magee, J. Electron. Mater. **20**, 279 (1990).
[68]M. Ishii, K. Nakashima, I. Tajima, and M. Yamamoto, Appl. Phys. Lett. **58**, 1378 (1991).
[69]C. Greenlief, S. Gates, and P. Holbert, Chem. Phys. Lett. **159**, 202 (1989).
[70]P. Gupta, V. Colvin, and S. George, Phys. Rev. B **37**, 8234 (1988).
[71]J. Proost, E. Kondoh, G. Vereecke, M. Heyns, and K. Maex, J. Vac. Sci. Technol., B **16**, 2091 (1998).
[72]J. Proost, M. Baklanov, K. Maex, and L. Delaey, J. Vac. Sci. Technol., B **18**, 303 (2000).
[73]Y. Kobayashi, Y. Shinoda, and K. Sugii, Jpn. J. Appl. Phys., Part 1 **29**, 1004 (1990).
[74]K. Ohkubo, Y. Igari, S. Tomoda, and I. Kusunoki, Surf. Sci. **260**, 44 (1992).
[75]M. D'evelyn, M. Nelson, and T. Engel, Surf. Sci. **186**, 75 (1987).
[76]J. Engstrom, D. Bonser, M. Nelson, and T. Engel, Surf. Sci. **256**, A541 (1991).
[77]M. Raschke, P. Bratu, and U. Hofer, Surf. Sci. **410**, 351 (1998).
[78]A. Endou, A. Stirling, R. Yamauchi, E. Broclawik, M. Kubo, A. Miyamoto, K. Nakamura, and M. Kitajima, Surf. Sci. **387**, 59 (1997).
[79]T. Hoshino, Phys. Rev. B **59**, 2332 (1999).
[80]T. Uchiyama, T. Uda, and K. Terakura, Surf. Sci. **474**, 21 (2001).

[81]M. Liehr, J. Lewis, and G. Rubloff, J. Vac. Sci. Technol., A **5**, 1559 (1987).
[82]J. Hannon, M. Bartelt, N. Bartelt, and G. Kellogg, Phys. Rev. Lett. **81**, 4676 (1998).
[83]N. Miyata, H. Watanabe, and M. Ichikawa, Phys. Rev. Lett. **84**, 1043 (2000).
[84]Y. Sun, D. Bonser, and T. Engel, Phys. Rev. B **43**, 14309 (1991).
[85]C. Cheng, S. Lucas, H. Gutleben, W. Choyke, and J. Yates, Jr., J. Am. Chem. Soc. **114**, 1249 (1992).
[86]J. Engstrom, M. Nelson, and T. Engel, Phys. Rev. B **37**, 6563 (1988).
[87]K. Oura, J. Yamane, K. Umezawa, M. Naitoh, F. Shoji, and T. Hanawa, Phys. Rev. B **41**, 1200 (1990).
[88]P. Lenahan and J. Conley, Jr., J. Vac. Sci. Technol., B **16**, 2134 (1998).